

High Frequency Quoting Under Liquidity Constraints

Aditya Nittur Anantha¹, Shashi Jain², Shivam Goyal³, and Dhruv Misra⁴

¹SigmaQuant Technologies Pvt. Ltd., Indian Institute of Science

²Indian Institute of Science

³AlgoQuant Fintech Ltd.

⁴AlgoQuant Fintech Ltd.

July 9, 2025

Abstract

Quoting algorithms are fundamental to electronic trading systems, enabling participants to post limit orders in a systematic and adaptive manner. In multi-asset or multi-contract settings, selecting the appropriate reference instrument for pricing quotes is essential to managing execution risk and minimizing trading costs. This work presents a framework for reference selection based on predictive modeling of short-term price stability. We employ multivariate Hawkes processes to model the temporal clustering and cross-excitation of order flow events, capturing the dynamics of activity at the top of the limit order book. To complement this, we introduce a Composite Liquidity Factor (CLF) that provides instantaneous estimates of slippage based on structural features of the book, such as price discontinuities and depth variation across levels. Unlike Hawkes processes, which capture temporal dependencies but not the absolute price structure of the book, the CLF offers a static snapshot of liquidity. A rolling voting mechanism is used to convert these signals into real-time reference decisions. Empirical evaluation on high-frequency market data demonstrates that forecasts derived from the Hawkes process align more closely with market-optimal quoting choices than those based on CLF. These findings highlight the complementary roles of dynamic event modeling and structural liquidity metrics in guiding quoting behavior under execution constraints.

1 Introduction

1.1 Motivation

High-frequency trading (HFT) has experienced substantial growth over the past decades, significantly influencing modern securities markets. In the U.S., HFT accounted for approximately 20% of equity trading in 2005, which surged to a peak of 60% by 2009 [1]. This rapid expansion is attributed to technological advancements and market participants' adoption of sophisticated quoting algorithms. These algorithms enable rapid placement and adjustment of buy and sell orders, reacting to real-time market data within microseconds. Such speed and efficiency are essential in today's liquid markets, where the volume of trading and competing algorithms necessitate swift responses to maintain a competitive edge [2].

Studies have further highlighted the significant role of HFT in price formation and liquidity provision. For instance, Clapham [3] emphasizes that high-frequency traders account for a substantial portion of overall price discovery and liquidity in modern securities markets. Additionally, Brogaard et al. [2] indicate that HFT firms contribute to over 50% of trading volume in U.S. equity markets, underscoring their dominant presence.

More recently, HFT has undergone a significant transformation, shifting from aggressive liquidity-taking strategies to more sophisticated quoting algorithms for execution. During the initial phase of HFT adoption, speed was the primary competitive advantage, with traders employing market order-based strategies to capture fleeting arbitrage opportunities. As low-latency infrastructure became widely available and competition intensified, these aggressive approaches faced diminishing returns due to increased transaction costs, market impact, and adverse selection risks. This evolution in market structure and competitive dynamics has prompted a shift toward execution strategies that prioritize efficiency, resilience, and adaptability. Quoting algorithms offer a sustainable and adaptive approach by intelligently placing and managing limit orders based on evolving market conditions. Rather than crossing the spread with market orders, these strategies shift the burden of research to predictive modeling of near term limit order book (LOB) state rather than the engineering objective of decreased latency. Market participants that use quoting algorithms to execute their trades aim to earn the spread by providing liquidity, thereby reducing execution costs and mitigating exposure to adverse selection. By incorporating predictive models on real-time market data, quoting algorithms allow participants to optimize execution quality, improve liquidity provision, and shift away from strategies that rely solely on latency as a competitive edge. Kearns et al. [4] highlighted that aggressive strategies often suffer from substantial execution costs and adverse price impacts, limiting their profitability. This necessitated a shift towards diversified approaches, particularly automated quoting strategies. By acting as market makers, traders using quoting strategies can maintain consistent income and reduce reliance on speed advantages [5].

At their core, quoting algorithms are automated systems that place and update limit orders on one or both sides of the LOB in response to market dynamics. These algorithms balance multiple objectives—such as reducing inventory risk, capturing the bid-ask spread, and maintaining quote competitiveness—while operating under stringent latency and reliability constraints. In the context of HFT, they are designed to react to microstructure-level events in real time, adjusting quoted prices and order sizes with high precision. Their effectiveness depends not only on speed, but also on the ability to anticipate short-term order flow and market conditions, making predictive modeling an essential component of modern quoting strategies [2].

In efficient markets, arbitrage opportunities are typically short-lived and require precise, rapid execution to be profitably exploited. As markets have become more electronic and competitive, the notion of arbitrage has expanded beyond simple price discrepancies to include statistical and structural inefficiencies that may persist over very short time horizons. Quoting algorithms are increasingly used as tools for arbitrage in this context—not to exploit obvious mispricings, but to identify and respond to subtle imbalances in supply and demand across related instruments or timeframes. This shift has laid the groundwork for more complex arbitrage frameworks involving multiple contracts and coordinated quoting logic.

Multi-contract arbitrage strategies further illustrate the evolution of HFT. These strategies exploit price discrepancies across correlated asset classes, leveraging complex instruments like calendar spreads, three-leg butterflies, and iron condors. For example, calendar spreads profit from time decay or volatility differences between futures or options contracts of the same underlying asset with different expiration dates [6]. Similarly, three-leg butterflies balance risk and reward during min-

imal price movement [7], while iron condors capture premium decay in range-bound markets [8]. Optimization techniques and dynamic rebalancing are crucial for managing such portfolios [9].

When employing a quoting algorithm for multi-contract arbitrage, a critical decision involves determining which contract or subset of contracts should be the reference price while posting limit orders on others to achieve the required spread. Quoting strategies address the inefficiencies of aggressive liquidity-taking execution. By conditionally placing quotes on a subset of assets while using others as references, these strategies aim to capture trader-defined spreads (S) while minimizing execution costs. Unlike reacting to market opportunities after they arise, quoting ensures that limit orders are already in place, increasing the likelihood of execution during favorable price movements. Typically, quoting algorithms place limit orders on a subset of contracts, with the price of the limit orders being a function of S and the reference price. Once the limit order is filled, the quoting algorithm executes an aggressive limit order¹ on the reference contract. This process assumes that the reference price remains stable during the time it takes for the limit order to be filled and the aggressive order to execute. Ensuring stability in the reference price during this time is crucial, as any significant changes could erode the profitability of the arbitrage trade.

In order to effectively control execution risk, market participants require methods to forecast which contract or subset of contracts is least likely to experience price changes during the critical execution interval. In this context, we explore two methods tailored for a fundamental example of multi-contract arbitrage: the futures calendar spread strategy. Calendar spreads, which involve offsetting positions in futures contracts of the same underlying asset with different expiration dates, are particularly sensitive to price dynamics [6]. Effective forecasting of stable reference contracts enhances the reliability and profitability of quoting strategies in these scenarios.

2 Literature and Existing Frameworks

The existing body of work provides frameworks and analyses to address the practical requirements of high-frequency quoting. [10] introduces a framework for optimal market making in an LOB, balancing profitability and inventory risk. [11] analyzes algorithmic trading strategies, including quoting algorithms, in *Algorithmic and High-Frequency Trading*. Similarly, [12] examines liquidity provision dynamics and quoting strategies' role in promoting market efficiency. In multi-asset trading, [13] highlights quoting algorithms' contributions to market efficiency and price discovery across multiple venues. High-frequency quoting strategies have been widely studied for their roles in market-making, arbitrage, and liquidity provision. These strategies target microstructure inefficiencies and short-term price movements while managing risks like slippage and adverse selection. Studies such as [10] and [14] provide optimal quoting frameworks for market-making, focusing on capturing the spread by quoting bid and ask prices simultaneously. In spread trading, [1] discusses exploiting relationships between correlated instruments, such as futures calendar and butterfly spreads. Effective execution algorithms are crucial for managing multi-leg trades efficiently while maintaining desired spreads. Probabilistic modeling techniques, like Hawkes processes, are powerful tools for analyzing market microstructure. [15] introduces these self-exciting point processes to model event clustering, such as trades and quote updates. Their temporal dependency modeling, as shown by [16], is valuable for forecasting order book dynamics. However, the decay kernel's choice

¹The National Stock Exchange (NSE) of India, prohibits market orders from being submitted by algorithmic trading systems, requiring all orders to have specified price limits. Consequently, our framework employs aggressive limit orders to ensure order execution within the permissible structure of the market.

significantly affects performance, motivating systematic optimization of kernel selection, as addressed in this paper. Real-time indicators based on order book data are integral to high-frequency quoting. [17] and [18] demonstrate how features like order book depth and imbalance inform trading decisions. This paper extends such approaches by introducing the Composite Liquidity Factor (CLF), which aggregates order book features into a single actionable metric. Although existing frameworks provide valuable foundations, they often lack adaptability to varying liquidity conditions. This paper bridges probabilistic forecasting with real-time decision-making by comparing the performance of Hawkes-based modeling and the CLF, offering a unified framework for optimizing high-frequency quoting strategies.

3 Contribution of This Paper

This paper introduces a novel framework for integrating liquidity measures and probabilistic modeling into high-frequency trading strategies. The contributions are summarized as follows:

- **Arrival ratio (ρ):** A high frequency measure derived from multivariate Hawkes processes that models order arrivals to estimate short-term price stability for reference contract selection.
- **Composite Liquidity Factor (CLF):** A high frequency liquidity metric derived from order book data, offering traders an actionable tool for decision-making in dynamic market environments.
- **Benchmark for evaluating quoting strategies:** We propose a benchmark against which a quoting strategy can be evaluated.
- **Empirical Validation:** Using tick-by-tick data from the Indian National Stock Exchange (NSE), we evaluate the proposed methodology’s impact on slippage reduction and spread capture.

4 Execution Structure and Reference Leg Selection Problem

Execution of calendar spread trades typically involves taking opposing positions in two futures contracts on the same underlying asset but with different expiry dates. While the theoretical spread between these contracts reflects cost-of-carry relationships, the realized execution cost is heavily influenced by the microstructure of the limit order book. In practice, algorithmic traders often employ *asymmetric quoting strategies*, where a limit order is placed on one leg of the spread (the quoting leg), and upon its execution, an aggressive order is immediately fired on the second leg (the reference leg) to complete the trade. This asymmetric execution introduces a time window—referred to as the *critical interval*—during which adverse price movements on the reference leg can lead to significant deviation from the intended spread. The central problem we address in this paper is the design of a reference leg selection strategy that minimizes expected slippage under such execution risk. This section formalizes the quoting framework, defines key variables, and motivates the need for a dynamic, data-driven approach to reference leg choice.

4.1 Quoting Mechanics and Execution Risk

A futures calendar spread strategy involves trading two futures contracts on the same underlying asset but with different expiration dates. The objective is to profit from changes in the price difference, or *spread*, between the near-term and far-term contracts. Table 1 presents the bid and ask prices of NIFTY futures contracts expiring in February 2022 and March 2022. The near-term contract (February) typically trades at a lower price, while the far-term contract (March) reflects higher prices, consistent with cost-of-carry models in futures markets.

Using an *aggressive liquidity-taking* execution strategy, the trader places *aggressive limit orders* to immediately execute trades by consuming available liquidity at the best bid and ask prices.¹

Remark 1. (On the Use of Aggressive Limit Orders)

At the National Stock Exchange (NSE) of India, algorithmic trading systems are prohibited from submitting market orders. Instead, execution is achieved through aggressive limit orders, which are limit orders posted with prices sufficiently favorable to ensure immediate execution against standing book liquidity. Throughout this paper, references to liquidity-taking strategies should be interpreted accordingly.

Suppose the trader anticipates that the spread between the two contracts will narrow over time due to market conditions, such as a reduced cost of carry or convergence in demand.

The trader initiates the calendar spread by:

- Buying the near-term (February) futures contract at the executed ask price $\tilde{p}_c^a(t_0) = 17,458.55$,
- Selling the far-term (March) futures contract at the executed bid price $\tilde{p}_n^b(t_0) = 17,514.20$,

at time $t = t_0$.

We adopt the following notational conventions throughout: $p(t)$ denotes the quoted limit order book price of a futures contract as a function of time t , with superscripts b and a indicating the bid and ask sides, respectively. The subscripts c and n , represent the current and the next month. $\tilde{p}(t)$ denotes an executed (traded) price at time t , distinguishing it from quoted limit order book prices. The trader defines a target spread S at the time of quoting, representing the desired price differential between legs. The realized (executed) spreads at entry and exit are denoted by \tilde{S}_{entry} and \tilde{S}_{exit} , respectively, reflecting the effective spread captured through actual trades. The net realized profit Π is computed as the difference between the entry and exit spreads. We let t_0 denote the time of spread entry and t_1 denote the time of spread exit.

The *entry spread* realized at time t_0 is computed as:

$$\tilde{S}_{\text{entry}} = \tilde{p}_n^b(t_0) - \tilde{p}_c^a(t_0), \quad (1)$$

$$\tilde{S}_{\text{entry}} = 17,514.20 - 17,458.55 = 55.65.$$

If the market evolves as expected and the spread narrows, the trader can exit the spread profitably. Suppose at time $t = t_1$, the February contract's bid price rises to $\tilde{p}_c^b(t_1) = 17,460.00$ and the March contract's ask price falls to $\tilde{p}_n^a(t_1) = 17,510.00$. Then, to close the position, the trader:

¹Throughout this paper, references to liquidity-taking strategies should be interpreted as involving aggressive limit orders, not market orders, in compliance with NSE regulations. See Remark 1.

- Sells the February contract at $\tilde{p}_c^b(t_1) = 17,460.00$,
- Buys back the March contract at $\tilde{p}_n^a(t_1) = 17,510.00$.

The *exit spread* realized at time t_1 is:

$$\begin{aligned}\tilde{S}_{\text{exit}} &= \tilde{p}_n^a(t_1) - \tilde{p}_c^b(t_1), \\ \tilde{S}_{\text{exit}} &= 17,510.00 - 17,460.00 = 50.00.\end{aligned}\tag{2}$$

The net realized profit per unit traded is given by:

$$\begin{aligned}\Pi &= \tilde{S}_{\text{entry}} - \tilde{S}_{\text{exit}}, \\ \Pi &= 55.65 - 50.00 = 5.65.\end{aligned}\tag{3}$$

This motivates a critical challenge in quoting strategies: identifying which contract or combination of contracts will exhibit the greatest price stability during the execution window, thereby maximizing the probability of achieving the desired spread.

4.2 Execution using quoting

The same spread trade can be executed through a quoting strategy. In this approach, the trader begins with a predefined target spread S . Rather than accepting the current market spread as fixed, the trader aims to minimize the cost of entry and maximize the profitability of the exit by selectively quoting one leg of the spread.

To execute the strategy, the price of one contract is designated as the *reference price*, and a limit order is placed on the other contract at a price derived as a function of the reference price and the target spread S . Upon the limit order being filled, a corresponding aggressive limit order (crossing the book) is triggered on the reference contract to complete the spread execution.

In pure liquidity-taking strategies, where immediate aggressive orders are fired on both legs simultaneously, the execution risk is considered negligible. This assertion is valid in markets that support atomic two-leg and three-leg Immediate-Or-Cancel (IOC) order types, which guarantee that either both legs execute simultaneously or neither leg executes. At the National Stock Exchange (NSE) of India, such IOC multi-leg orders are supported. Consequently, when using simultaneous liquidity-taking across legs, the execution of the trader's view on the spread occurs with atomicity, and execution risk can be considered zero.

In quoting strategies, however, execution risk is non-zero. This arises because of the latency between the limit order on the quoting leg being filled and the aggressive limit order on the reference leg being fired and executed. During this time window, the reference price may change adversely.

As a result, the realized spread at time t , denoted $\tilde{S}(t)$, may differ from the trader's intended spread S . In certain market conditions such as contango, the farther-month futures price may trade below the nearer-month price, leading to a negative target spread.² The slippage associated with quoting, denoted $\delta_S(t)$, is defined as:

$$\delta_S(t) = |S - \tilde{S}(t)|.\tag{4}$$

²See Remark 2 for a discussion on contango markets and reverse spreads.

A critical aspect of quoting across contracts is the choice of which contract to reference. The choice directly impacts both the realized cost at entry and the realized profit at exit. The core forecasting problem addressed in this paper is selecting the reference leg that minimizes the probability of unfavorable price changes during the execution window.

Remark 2. (*On Reverse Arbitrage and Contango Markets*)

In certain market conditions such as contango, the futures price of a farther-month contract may trade below that of a nearer-month contract. This results in a negative intended spread S for calendar spread strategies. The slippage definition $\delta_S(t) = |S - \hat{S}(t)|$ naturally accommodates both positive and negative target spreads.

4.3 Execution using limit orders

Market makers frequently employ quoting strategies that involve placing limit orders on both the bid and ask sides of the limit order book (LOB), aiming to profit from short-term fluctuations in the bid-ask spread—especially during phases of spread expansion or contraction. However, in the context of futures rollover trades, simultaneously quoting both legs of a multi-contract strategy increases execution risk. The resulting fill asymmetry can lead to a significant deviation between the realized spread $\hat{S}(t)$ and the trader’s intended spread S , reflected in higher slippage $\delta_S(t)$.

Another critical consideration when designing quoting strategies is whether the objective is to minimize execution risk alone, or whether it must also meet minimum trading volume constraints over time. While the framework presented in this paper can be extended to symmetric quoting across multiple contracts, our focus is specifically on *asymmetric multi-contract quoting strategies*, in which limit orders are placed only on a subset of contracts and priced using reference prices derived from a disjoint subset.

Impact of Reference Leg Selection on Execution Slippage

This subsection presents a concrete example of how the choice of reference leg—i.e., which contract’s price is used to trigger the market order—can significantly affect the realized spread and slippage in a calendar spread quoting strategy.

We consider two futures contracts on the same underlying: the *current month contract* (denoted by subscript c) and the *next month contract* (subscript n). The trader wishes to enter a spread trade at time t_0 with a mandated spread of $S(t_0) = 58.5$ INR per contract.

Time Convention:

- t_0 : time of initial quote placement.
- t_1 : time when the quoting leg limit order is executed.
- t_2 : time when the reference leg (aggressive order) is executed.

The interval $[t_1, t_2]$ is referred to as the *critical interval*.

Notation Convention:

- $p_k^b(t)$: best bid price of contract $k \in \{c, n\}$ at time t
- $p_k^a(t)$: best ask price of contract k at time t
- $S^{(r)}(t)$: spread implied by reference leg $r \in \{c, n\}$ at time t

- $\tilde{S}^{(r)}(t_2)$: realized spread at execution
- $\delta_S^{(r)}(t_2) = |\tilde{S}^{(r)}(t_2) - S(t_0)|$: slippage

All prices and spreads are expressed in INR per contract.

Remark 3. (On Slippage and Execution Timing)

The time difference between the execution of the quoting leg and the reference leg is called the critical interval. During this interval, the top-of-book price on the reference leg may change. This affects the realized spread $\tilde{S}^{(r)}(t_2)$, causing deviation from the trader's mandated spread $S(t_0)$. We define the slippage incurred as:

$$\delta_S^{(r)}(t_2) = \left| \tilde{S}^{(r)}(t_2) - S(t_0) \right|$$

A positive slippage implies favorable price movement during execution; a negative value implies a cost.

Top of Book at t_0

Table 1: Top 5 levels of the LOB at time t_0 for NIFTY February and March Futures

NIFTY February 2022				NIFTY March 2022			
Bid	Qty	Ask	Qty	Bid	Qty	Ask	Qty
17455	50	17458.55	50	17514.2	50	17516.5	150
17450	50	17459.65	50	17510.2	150	17516.55	50
17401.1	100	17459.95	100	17510.1	100	17516.7	50
17376	800	17460	550	17509.1	150	17517.2	50
17355	100	17475	250	17503.6	50	17523.4	200

From this, the two implied spreads are:

$$\begin{aligned}
S^{(c)}(t_0) &= p_n^b(t_0) - p_c^b(t_0) \\
&= 17514.2 - 17455 \\
&= 59.2
\end{aligned} \tag{5}$$

$$\begin{aligned}
S^{(n)}(t_0) &= p_n^a(t_0) - p_c^a(t_0) \\
&= 17516.5 - 17458.55 \\
&= 57.95
\end{aligned} \tag{6}$$

Case 1: Current Month as Reference Leg:

In this setup, the trader designates the *current month contract* as the reference leg. A buy limit order is placed on the *next month contract* at time t_0 , quoting the best available ask price of $p_n^a(t_0) = 17514.2$. This order is executed at time t_1 .

Following this execution, at time t_2 , the trader fires an *aggressive limit order* to sell the current month contract. During the *critical interval* $[t_1, t_2]$, the top bid on the current month leg improves from 17455 to 17458. Consequently, the aggressive order is executed at the updated price $p_c^b(t_2) = 17458$.

The spread realized under this execution path, denoted $\tilde{S}^{(c)}(t_2)$, is calculated as the difference between the bid on the next month leg (observed at t_1) and the updated bid on the reference leg (current month) at t_2 . This spread is 56.2 INR, leading to a slippage of 2.3 INR compared to the mandated spread of 58.5 INR.

Despite initially observing a wider possible spread, the trader incurs higher slippage due to adverse price movement during the critical interval.

Table 2: LOB snapshots when current month is the reference leg

NIFTY March 2022 (t_1)				NIFTY February 2022 (t_2)			
Bid	Qty	Ask	Qty	Bid	Qty	Ask	Qty
17514.2	50	17514.2	50	17458	50	17458.55	50
17510.2	50	17516.5	150	17455	50	17459.65	50
17510.1	150	17516.55	50	17450	50	17459.95	100
17509.1	100	17516.7	50				

$$\begin{aligned}
\tilde{S}^{(c)}(t_2) &= p_n^b(t_1) - p_c^b(t_2) \\
&= 17514.2 - 17458 \\
&= 56.2
\end{aligned} \tag{7}$$

$$\begin{aligned}
\delta_S^{(c)}(t_2) &= |56.2 - 58.5| \\
&= 2.3 \text{ INR per contract}
\end{aligned} \tag{8}$$

Case 2: Next Month as Reference Leg:

In this alternative configuration, the trader chooses the *next month contract* as the reference leg. A buy limit order is placed on the *current month contract* at time t_0 , quoting the best available ask price of $p_c^a(t_0) = 17458.55$. This order is filled at time t_1 .

At t_2 , the trader fires an aggressive limit order on the next month contract to sell at market. During the critical interval, the top ask price on the next month contract shifts slightly from 17516.5 to 17516.55, reflecting minor upward movement. The order is thus executed at the updated price $p_n^a(t_2) = 17516.55$.

The realized spread $\tilde{S}^{(n)}(t_2)$, computed as the difference between the ask on the reference leg (next month) at t_2 and the ask on the quoting leg (current month) at t_1 , equals 58.0 INR. This results in a slippage of only 0.5 INR from the mandated spread.

Although the next month leg had a slightly narrower spread at t_0 , the higher short-term stability during the critical interval led to significantly lower execution risk.

Table 3: LOB snapshots when next month is the reference leg

NIFTY February 2022 (t_1)				NIFTY March 2022 (t_2)			
Bid	Qty	Ask	Qty	Bid	Qty	Ask	Qty
17458.55	50	17458.55	50	17514.2	50	17516.55	50
17455	50	17459.65	50	17510.2	150	17516.7	50
17450	50	17459.95	100	17510.1	100	17517.2	50

$$\begin{aligned}
\tilde{S}^{(n)}(t_2) &= p_n^a(t_2) - p_c^a(t_1) \\
&= 17516.55 - 17458.55 \\
&= 58.0
\end{aligned} \tag{9}$$

$$\begin{aligned}
\delta_S^{(n)}(t_2) &= |58.0 - 58.5| \\
&= 0.5 \text{ INR per contract}
\end{aligned} \tag{10}$$

Summary and Interpretation

Table 4: Reference Leg Pricing Path

Ref. Leg	Quoted Price	Exec. Price	Ref Price (t_0)	Ref Exec (t_2)
Current Month ($r = c$)	17514.2	17514.2	17455	17458
Next Month ($r = n$)	17458.55	17458.55	17516.5	17516.55

Table 5: Realized Spread and Slippage

Ref. Leg	Realized Spread	Slippage (INR)
Current Month ($r = c$)	56.2	2.3
Next Month ($r = n$)	58.0	0.5

Although the initial spread was wider when the current month was selected as the reference leg, the final realized spread was lower due to price movement during the critical interval, resulting in higher slippage. Conversely, the next month leg provided better price stability, despite a narrower initial spread, and resulted in lower slippage.

This highlights the core insight: short-term stability of the reference leg is more important than instantaneous spread width when minimizing execution risk.

5 Problem Formulation: Optimal Reference Leg Selection

The preceding empirical comparison illustrates that the choice of reference leg in a calendar spread quoting strategy materially affects the realized spread and slippage. Specifically, even when the

initial observed spread favors one contract, short-term price stability during the critical interval can dominate realized execution outcomes. Motivated by these observations, we now formalize the reference leg selection problem as a dynamic decision-making process. At each quoting decision point, the trader must select the contract to treat as the reference leg based on observable market conditions, with the objective of minimizing expected slippage relative to a mandated spread constraint. Unlike classical optimization problems, this selection is guided by statistical methods and empirical characteristics of the limit order book rather than by solving an explicit minimization problem. This formulation captures the execution asymmetry inherent in quoting strategies and provides the foundation for systematic reference leg selection based on real-time market data.

Let $\mathcal{W} = \{w^{(1)}, w^{(2)}, \dots\}$ be a collection of non-overlapping evaluation intervals of the form $w = [w_1, w_2)$, where w_1 and w_2 denote the start and end of each interval respectively.

Iterating over each interval in \mathcal{W} , we consider two classes of filters that guide quoting decisions at time w_1 :

- Filters $\mathcal{G}^T(w)$ that act on the stream of trades and quotes observed strictly prior to the start of the interval.
- Filters $\mathcal{G}^B(w)$ that operate on the order book snapshot observed at the start of the interval.

Each filter selects or scores relevant inputs from its respective domain, producing a filtered representation that will be used to assess the quoting viability of each contract leg.

Each filter is paired with a quoting function that maps the filtered representation to a real-valued score for each candidate leg. The tick-based quoting function \mathcal{Q}^T operates on the output of $\mathcal{G}^T(w)$, while the book-based quoting function \mathcal{Q}^B operates on the output of $\mathcal{G}^B(w)$.

Each quoting function returns a real-valued estimate of expected slippage for each leg $r \in \{c, n\}$, and selects the leg with the smaller value:

$$\mathcal{Q}^T(w) := \arg \min_{r \in \{c, n\}} \mathbb{E}[\delta_S^{(r)}(w_2) \mid \mathcal{G}^T(w)] \quad \forall w \in \mathcal{W} \quad (11)$$

$$\mathcal{Q}^B(w) := \arg \min_{r \in \{c, n\}} \mathbb{E}[\delta_S^{(r)}(w_2) \mid \mathcal{G}^B(w)] \quad \forall w \in \mathcal{W} \quad (12)$$

Here, $\delta_S^{(r)}(w_2)$ denotes the realized slippage incurred on leg r at the end of the interval, and the filters $\mathcal{G}^T(w)$ and $\mathcal{G}^B(w)$ encode the information available at decision time.

The quoting decisions are finally expressed as binary indicators:

$$\chi^T(w) := \mathbb{I}\{\mathcal{Q}^T(w) = n\}, \quad \chi^B(w) := \mathbb{I}\{\mathcal{Q}^B(w) = n\} \quad (13)$$

where a value of 1 indicates that the quoting rule recommends the next-month leg, and 0 indicates the current-month leg.

We denote by $\chi^m(w) \in \{0, 1\}$ the market-optimal reference leg decision for interval w , defined as the choice that yields the lowest realized slippage in hindsight. This benchmark provides a reference against which to evaluate the quality of decisions made by each quoting rule.

Problem 1.2 (Evaluation of Reference Leg Selection Rules).

Given a collection of evaluation intervals \mathcal{W} , and binary-valued quoting decisions $\chi^T(w)$, $\chi^B(w)$, and the market-optimal reference decision $\chi^m(w) \in \{0, 1\}$, define the agreement score:

$$\mathcal{A}(\chi, \chi^m) := \frac{1}{|\mathcal{W}|} \sum_{w \in \mathcal{W}} \mathbb{I}\{\chi(w) = \chi^m(w)\}$$

The objective is to compute and compare the agreement scores $\mathcal{A}(\chi^T, \chi^m)$ and $\mathcal{A}(\chi^B, \chi^m)$.

6 Methodology

The decision rules introduced in Problem 1.2 are evaluated against an oracle benchmark that reflects the most favorable realized execution observed in hindsight. In the context of machine learning, an oracle typically refers to an idealized entity or function that provides the correct label or decision for each input. Here, the oracle decision $\chi^m(w)$ identifies the reference leg—either current or next month—that would have minimized realized slippage within a given evaluation window w . It serves as a ground truth label for scoring the performance of quoting strategies based on observable signals. The methodology outlined in this section implements the decision rules $\chi^T(w)$ and $\chi^B(w)$, instantiates the oracle decision $\chi^m(w)$ from tick data, and computes the agreement score defined in Problem 1.2 as the primary evaluation metric.

6.1 Execution Design and Quoting Framework

Let F_c be the futures contract expiring in the current month (with price $p_c(t)$ at time t), and let F_n be the contract expiring in the next month (with price $p_n(t)$). Let q denote the quantity to roll over, and S denote the maximum acceptable rollover cost (price difference per unit). Executing a rollover trade then entails selling q units of F_c and buying q units of F_n , under the constraint $p_n(t) - p_c(t) \leq S$, ensuring total cost remains within the threshold S .

In an efficient, arbitrage-free market with risk-free rate R , the prices satisfy the theoretical cost-of-carry relation: $p_n(t) = e^{Rt} p_c(t)$. This leads to the theoretical spread:

$$S_m(t) = p_c(t)(e^{Rt} - 1),$$

which may deviate in practice due to mispricing or market frictions. These frictions motivate quoting strategies that dynamically adjust order prices to maintain execution costs below S .

We consider two quoting configurations:

Case 1: Using F_c as reference. The price $p_c^r(t)$ is computed as the VWAP over the top ν levels on the bid side of F_c 's LOB:

$$p_c^r(t) = \frac{\sum_{i=1}^{\nu} p_c^{b,i} q_c^{b,i}}{\sum_{i=1}^{\nu} q_c^{b,i}},$$

with quoting price on F_n set to:

$$p_n^l(t) = S - p_c^r(t).$$

Case 2: Using F_n as reference. The price $p_n^r(t)$ is derived similarly from the ask side of F_n 's LOB:

$$p_n^r(t) = \frac{\sum_{i=1}^{\nu} p_n^{a,i} q_n^{a,i}}{\sum_{i=1}^{\nu} q_n^{a,i}},$$

with quoting price on F_c set to:

$$p_c^l(t) = p_n^r(t) - S.$$

The realized spread $\tilde{S}(t)$ is computed from the resulting trade prices after quoting and aggressive leg execution. A key design decision is determining which contract to use as the reference leg, since this impacts execution cost and slippage.

6.2 Tick-Based and Book-Based Reference Leg Selection

We now formalize two reference leg selection rules that instantiate the quoting framework introduced in Section 5.

Tick-based quoting rule. For each interval $w \in \mathcal{W}$, we define a tick-based quoting rule that estimates the expected slippage of each leg using filtered trade and quote activity observed strictly prior to the quoting time w_1 :

$$\mathcal{Q}^T(w) := \arg \min_{r \in \{c,n\}} \mathbb{E} \left[\delta_S^{(r)}(w_2) \mid \mathcal{G}^T(w) \right] \quad (14)$$

The quoting decision is then encoded as a binary rule:

$$\chi^T(w) := \mathbb{I} \{ \mathcal{Q}^T(w) = n \} \quad (15)$$

Book-based quoting rule. Similarly, for each $w \in \mathcal{W}$, we define a book-based quoting rule that uses the order book snapshot observed at time w_1 to evaluate expected slippage:

$$\mathcal{Q}^B(w) := \arg \min_{r \in \{c,n\}} \mathbb{E} \left[\delta_S^{(r)}(w_2) \mid \mathcal{G}^B(w) \right] \quad (16)$$

with associated decision function:

$$\chi^B(w) := \mathbb{I} \{ \mathcal{Q}^B(w) = n \} \quad (17)$$

These rules implement quoting strategies presented in 5 based on real-time market observables, where tick-based filters aggregate historical event data, and book-based filters extract instantaneous liquidity conditions. The decision outcome in each case is a binary indicator for whether to quote on the next-month leg.

7 Benchmarking Framework for Quoting Strategies

To compare quoting rules, we define a market-derived oracle decision $\chi^m(w) \in \{0,1\}$ based on actual executed spread trades.

Let $\mathcal{E} = \{T, C, \text{PDM}\}$ denote the set of event types observed in tick data, where T represents trades, C represents cancellations, and PDM denotes price downward modifications.

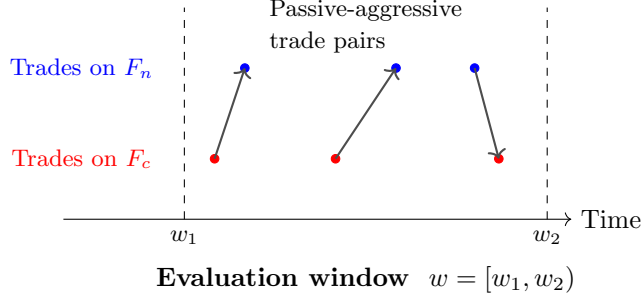


Figure 1: Illustration of benchmark construction using passive-aggressive trade pairs within interval $w = [w_1, w_2)$. The first-leg execution determines the oracle decision $\chi^m(w)$.

The tick-based filter $\mathcal{G}^T(w)$ returns the set of valid passive-aggressive trade pairs identified within the interval $w = [w_1, w_2)$, extracted from tick history and used to construct the benchmark reference leg decision.

Remark 4. (Trade-Only Basis for Benchmark Construction)

Only Trade events are used to construct the benchmark decision $\chi^m(w)$. Events of type Cancellation or Price Downward Modification are excluded from the filtered set $\mathcal{G}^T(w)$, ensuring that benchmarking reflects executed spread trades alone.

For each pair $(t_1, t_2) \in \mathcal{G}^T(w)$, the realized spread is:

$$\tilde{S}_m(t) = p_n^{b,T}(t_2) - p_c^{a,T}(t_1)$$

, where T represents event-type Trade. The oracle decision is:

$$\chi^m(w) := \begin{cases} 1 & \text{if } F_c \text{ was traded first (ref leg is } F_n) \\ 0 & \text{if } F_n \text{ was traded first (ref leg is } F_c) \end{cases}$$

Each quoting rule $\chi(w) \in \{\chi^T(w), \chi^B(w)\}$ is compared to $\chi^m(w)$ using the agreement score:

$$\mathcal{A}(\chi, \chi^m) := \frac{1}{|\mathcal{W}|} \sum_{w \in \mathcal{W}} \mathbb{I}\{\chi(w) = \chi^m(w)\}$$

Remark 5. (On Quantity Normalization)

All observed calendar spread trades in $\mathcal{G}^T(w)$ are evaluated using the minimum tradable quantity permitted by the venue. This ensures that the realized spread $\tilde{S}_m(t)$ reflects slippage on a per-unit basis, independent of execution size.

In plain terms, the oracle label $\chi^m(w)$ is determined by finding actual calendar spread trades in the tick data. These trades are identified as passive-aggressive trade pairs in opposite contracts, occurring within a short critical interval. We retain only those trades that match rollover logic—buying F_n , selling F_c —and compute the realized spread for each. The lowest spread in the window determines the oracle decision based on which leg executed first. The complete filtered set of such trades is denoted $\mathcal{G}^T(w)$, and all benchmarking is grounded in this empirically observed structure.

8 Data

This study uses tick-by-tick (TBT) market data from the National Stock Exchange (NSE) of India, collected on February 7, 2022, for NIFTY futures contracts.³ The dataset includes two instruments: the current-month contract expiring on February 24, 2022 (F_c) and the next-month contract expiring on March 31, 2022 (F_n). Both contracts exhibit high liquidity and dense tick arrival activity, enabling fine-grained execution modeling.

Each tick is one of four event types: **NEW** (order addition), **MODIFY** (order revision), **CANCEL** (order withdrawal), and **TRADE** (execution). These types are used to extract features relevant to quoting behavior and limit order book dynamics. The minimum tick size for NIFTY futures is INR 0.05, as mandated by NSE.

The data is segmented into a collection of evaluation windows $\mathcal{W} = \{w = [w_1, w_2]\}$, where each window spans a short time interval (e.g., 100 milliseconds) aligned with the quoting decision frequency. For each $w \in \mathcal{W}$, we apply two distinct classes of filters:

- The tick-based filter $\mathcal{G}^T(w)$ operates on the stream of trades and quotes observed strictly prior to the quoting time w_1 .
- The book-based filter $\mathcal{G}^B(w)$ extracts features from the limit order book snapshot observed exactly at time w_1 .

These filters produce real-valued representations of prevailing market conditions that serve as inputs to the quoting rules defined in Section 5.

Tick-derived features. For each evaluation window $w \in \mathcal{W}$, the tick-based filter $\mathcal{G}^T(w)$ encodes summary statistics of recent trade and quote activity observed strictly prior to the quoting time w_1 . These features include:

- Count of executed trades (**TRADE** events).
- Count of order cancellations (**CANCEL** events).
- Count of price-worsening quote updates (**MODIFY** events where the best price deteriorates).
- Total number of tick events, inclusive of all above types.

Book-derived features. For each interval $w \in \mathcal{W}$, the book-based filter $\mathcal{G}^B(w)$ extracts directional liquidity indicators from the limit order book snapshot observed at time w_1 . These features are computed separately for each contract leg and for each relevant side of the book (bid or ask), based on whether the leg is expected to be lifted or hit under the quoting convention.

Specifically, we extract:

- Price at each level $p^{b,i}, p^{a,i}$, for $i = 1, \dots, \nu$
- Quantity available at each level $q^{b,i}, q^{a,i}$, for $i = 1, \dots, \nu$

These level-wise features are later used to construct directional liquidity measures such as the Composite Liquidity Factor (CLF), introduced in a subsequent section, which serve as inputs to the book-based quoting rule \mathcal{Q}^B .

³All exchange specifications and market microstructure rules referenced in this study reflect those in effect as of March 2022, corresponding to the period from which the data was collected.

Data scale. Table 6 reports the total number of ticks recorded for each contract on February 7, 2022. The substantial volume supports the evaluation of quoting strategies at a high temporal resolution.

Contract	Date	Number of ticks/day
Futures (G22)	07/02/2022	49,828,303
Futures (H22)	07/02/2022	16,349,197
Futures (H22)	10/03/2022	42,000,613
Futures (J22)	10/03/2022	9,562,649
Futures (H22)	24/03/2022	43,306,045
Futures (J22)	24/03/2022	18,238,164

Table 6: Data Statistics (The code in the parenthesis denotes expiry in the format: <month_code><year>)

A sample from the processed tick data is provided in the appendix for illustration.

9 Forecasting Execution Risk with Multivariate Hawkes Processes

The preceding section introduced the structure of tick-level events segmented by order book side and event type. We now present a predictive framework that leverages these microstructural observations to forecast execution risk across candidate reference legs. Specifically, we construct forward-looking arrival ratios using multivariate Hawkes processes and use them to infer a reference leg decision. This model-based strategy complements the reactive rule-based approaches presented earlier and provides a direct forecasting proxy for the oracle decision $\chi^m(w)$ introduced in Problem 1.2.

9.1 Forecasting Objective and Model Structure

Let $\mathcal{E} = \{T, C, PDM\}$ denote the set of reference-impacting event types: trades, cancellations, and downward price modifications. Let $Y = \{b, a\}$ represent the bid and ask sides of the order book, and $X \in \{c, n\}$ index the current and next-month contracts. Define the joint index set $\mathcal{I} = \mathcal{E} \times Y$.

Our goal is to forecast, over a forward interval $(\tau, \tau + \xi]$, the number of reference-impacting events $\tilde{N}_{(\tau, \tau + \xi]}^{X, Y, r}$ and the total number of events $\tilde{N}_{(\tau, \tau + \xi]}^{X, Y}$. From these, we compute the arrival ratio:

$$\rho_{(\tau, \tau + \xi]}^{X, Y} = \frac{\tilde{N}_{(\tau, \tau + \xi]}^{X, Y, r}}{\tilde{N}_{(\tau, \tau + \xi]}^{X, Y}} \quad (18)$$

Given that spread execution involves selling F_c and buying F_n , the ask side of F_c and the bid side of F_n are relevant. We therefore define the reference leg decision based on the forecasted arrival ratios:

$$\tilde{\chi}_{(\tau, \tau + \xi]} = \mathbb{I} \left\{ \rho_{(\tau, \tau + \xi]}^{c, a} \geq \rho_{(\tau, \tau + \xi]}^{n, b} \right\} \quad (19)$$

To maintain consistency with the decision framework introduced in Problem 1.2, we denote this forecasting-driven rule as $\mathcal{Q}^{\mathcal{H}}$, with its output defined as:

$$\chi^{\mathcal{H}}(w) := \tilde{\chi}_{(\tau, \tau + \xi]} = \mathbb{I} \left\{ \rho_{(w)}^{c,a} \geq \rho_{(w)}^{n,b} \right\}, \quad \text{where } w = (\tau, \tau + \xi]$$

Here, $\mathcal{Q}^{\mathcal{H}}$ maps estimated arrival ratios to a binary reference leg decision over window $w \in \mathcal{W}$. This rule completes the triad of decision functions $\{\mathcal{Q}^{\mathcal{T}}, \mathcal{Q}^{\mathcal{B}}, \mathcal{Q}^{\mathcal{H}}\}$, all evaluated against the market oracle $\chi^m(w)$ using the agreement score defined in Problem 1.2.

Formal Definition: Hawkes-Derived Feature Mapping.

For each interval $w = [w_1, w_2) \in \mathcal{W}$, let $\mathcal{G}^{\mathcal{H}}(w) \in \mathbb{R}^2$ denote the filtered representation obtained by simulating a fitted Hawkes model on recent tick data to estimate directional arrival ratios. Define:

$$\begin{aligned} \tilde{N}_{(w)}^{X,Y} & \quad \text{Simulated total Hawkes event counts on } w \\ \tilde{N}_{(w)}^{X,Y,r} & \quad \text{Simulated events attributed to leg } r \in \{c, n\} \\ \rho_{(w)}^{X,Y} & := \frac{\tilde{N}_{(w)}^{X,Y,r}}{\tilde{N}_{(w)}^{X,Y}} \\ \mathcal{G}^{\mathcal{H}}(w) & := \left(\rho_{(w)}^{c,a}, \rho_{(w)}^{n,b} \right) \\ \mathcal{Q}^{\mathcal{H}}(w) & := \arg \min_{r \in \{c, n\}} \rho^{r,s}(w) \\ \chi^{\mathcal{H}}(w) & := \mathbb{I} \{ \mathcal{Q}^{\mathcal{H}}(w) = n \} \end{aligned}$$

where $\rho^{r,s}(w)$ represents the simulated relative arrival intensity for quoting side s of leg r , and n refers to the next-month contract.

The above formalization defines the Hawkes-based decision rule $\chi^{\mathcal{H}}(w)$ as a function of simulated forward event counts derived from fitted multivariate Hawkes models. By comparing the relative frequency of reference-price-impacting events across book sides, this approach translates microstructural event flow forecasts into a structured quoting decision. This provides a direct, data-driven proxy for short-term execution stability under each reference leg and can be evaluated against the market-optimal decision $\chi^m(w)$.

Modeling Remark

This decision rule $\chi^{\mathcal{H}}(w)$ serves as a forecasting-based analog of the oracle decision $\chi^m(w)$. It selects the contract whose book side is expected to exhibit fewer reference-price-impacting events, thus offering more stable execution.

9.2 Multivariate Hawkes Process for Event Forecasting

We model reference-impacting events using multivariate Hawkes processes [15]. For each contract X and side Y , we define a D -dimensional Hawkes process indexed by $i \in \mathcal{I}$. The intensity λ_t^i evolves

as:

$$\lambda_t^i = \mu^i + \sum_{j=1}^D \int_0^t \phi_{ij}(t-s) dN_s^j \quad (20)$$

where $\phi_{ij}(t)$ captures the excitation effect of events of type j on type i .

Following [19], we estimate separate Hawkes models for:

- Reference-impacting events only $N^{X,Y,r}$
- All events $N^{X,Y}$

Each model is estimated on a rolling basis over historical windows $(\tau - h, \tau]$, yielding fitted kernels $\hat{\Phi}^{X,Y,r}$ and $\hat{\Phi}^{X,Y}$.

9.3 Estimation and Simulation Procedure

The accuracy of short-term event forecasts under the Hawkes framework depends critically on the choice of kernel function $\phi_{ij}(t)$, which encodes the temporal excitation effect of past events. We evaluate both parametric and non-parametric approaches to kernel estimation, balancing model interpretability, estimation stability, and flexibility of fit.

Parametric kernels include the exponential and sum-of-exponentials forms, whose functional structures are shown in Table 7. These allow for low-dimensional maximum likelihood estimation and are widely used in market microstructure applications due to their analytical tractability.

Non-parametric kernels, by contrast, do not assume a fixed functional form. Instead, we consider two classes of non-parametric estimators: (i) the *expectation-maximization* (EM) method, which iteratively estimates a discretized kernel by maximizing a latent-variable likelihood, and (ii) the *conditional law approach*, which reconstructs the kernel by inverting the conditional intensity relation from observed event times. These methods provide flexible approximations of $\phi_{ij}(t)$, allowing for data-driven recovery of potentially complex excitation structures.

Table 7: Evaluated Parametric Kernels

Kernel Type	Functional Form	Method
Exponential	$\alpha e^{-\beta t}$	TICK MLE
Sum of exponentials	$\sum_u \alpha_u e^{-\beta_u t}$	TICK MLE

The estimation and simulation procedures employed here closely follow those developed in our earlier work [19]. The present formulation adapts those methods to forecast arrival ratios for reference-impacting events, enabling their integration into a structured decision rule.

Hawkes kernels are estimated via maximum likelihood using the method of [20]. For parametric kernels, we use exponential and sum-of-exponentials forms. Non-parametric estimation follows [21, 22]. Simulated event sequences are generated using Ogata’s thinning method [23].

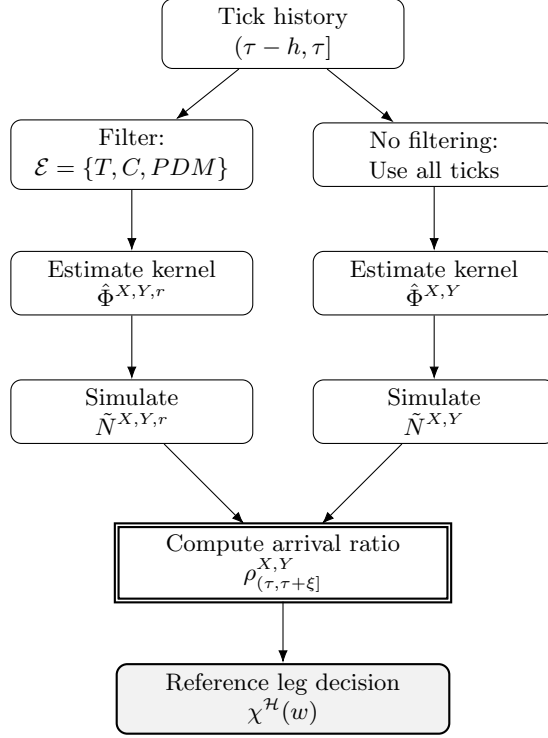


Figure 2: Forecasting decision pipeline: kernel estimation, simulation, arrival ratio computation, and final decision $\chi^{\mathcal{H}}(w)$.

9.4 Forecast Evaluation and Model Selection

To assess kernel performance, we compare simulated distributions $\tilde{\mathcal{D}}_{\omega}^{X,m}$ of forecasted counts against realized counts $N_{(\tau,\tau+\xi]}^{X,Y,r}$, computing the log-likelihood loss:

$$\ell^{X,m} = - \sum_{j=1}^T \log \mathbb{P} \left(N_{\omega_j}^{X,Y,r} \mid \tilde{\mathcal{D}}_{\omega_j}^{X,m} \right) \quad (21)$$

Model selection is based on the test for superior predictive ability (SPA) [24], which compares competing kernels under common evaluation metrics while controlling for multiple testing.

The best-performing kernel $\hat{\Phi}^*$ is used for all subsequent simulations. The resulting forecasting-based decision rule $\chi^{\mathcal{H}}(w)$ is benchmarked against the oracle decision $\chi^m(w)$ using the agreement score defined in Problem 1.2.

Summary: Integration into Evaluation Framework

The Hawkes-based arrival ratio forecast yields a reference leg decision that anticipates short-term slippage risk. This decision is validated by comparing its alignment with the oracle decision across evaluation windows, allowing rigorous benchmarking against book- and tick-based quoting rules.

10 Reference Leg Selection via Order Book Liquidity Profiles

The preceding section developed a reference leg selection rule based on intensity forecasts derived from tick history using multivariate Hawkes processes. In contrast, we now consider a structurally simpler approach that relies entirely on the instantaneous state of the order book—specifically, the slope and depth of price levels on each side. While the Hawkes-based method models temporal dependencies in event arrivals, the order-book-state-based method assumes that key execution-relevant information is already embedded in the current liquidity profile. This contrast implicitly reflects two different informational assumptions: one emphasizes historical flow; the other emphasizes present structure. We make no claims about market efficiency, but use this contrast to motivate an alternative, real-time computable quoting rule based on liquidity discontinuities.

While recent models of limit order book dynamics—particularly those based on multivariate Hawkes processes—offer detailed descriptions of market microstructure, their practical adoption in high-frequency trading (HFT) remains limited. This gap stems primarily from the computational complexity inherent in estimating and updating such models in real time. Studies such as Chavez-Demoulin and McGill [25] emphasize the intensive nature of maximum likelihood estimation for Hawkes processes, which can render them unsuitable for latency-sensitive HFT environments. Real-time simulation of event intensities, which depend on the full event history, further adds to the processing burden, especially in multivariate settings where many event types and cross-excitation terms are involved.

The trade-off between model expressiveness and tractability becomes especially pronounced in quoting strategies that require continuous adaptation. Consequently, practical HFT systems often rely on simplified heuristics or lightweight statistical indicators that can be computed at sub-millisecond timescales. This motivates the development of forecasting frameworks that retain the interpretability and structure of LOB-aware models—such as those based on Hawkes processes—while offering tractability and responsiveness suitable for real-time quoting systems [19]. However, a key limitation of this framework is its exclusion of the absolute price levels present in the LOB. While the Hawkes model effectively represents the timing and interaction of events, it treats the price itself as exogenous and does not integrate its magnitude into the structure of the model.

This modeling lacuna has important implications when the objective is to identify the more stable reference contract for execution. In particular, discontinuities in the price levels across the order book can lead to non-trivial slippage, especially when order sizes exceed the available liquidity at the best quotes. For example, in Table 1, the bid side of the NIFTY February 2022 futures contract shows a significant drop from INR 17450 at price level 2 to INR 17401.1 at price level 3, on the bid side,—a INR 48.9 decline. A market order large enough to consume the top two bid levels would thus incur a sharp execution cost due to this gap.

The magnitude of such price-level drops is crucial for modeling expected slippage and, by extension, for determining the optimal reference contract under liquidity constraints. The current Hawkes-based framework, however, is not equipped to capture this dimension. This limitation suggests the need for an augmented model that accounts for price slope and liquidity profile.

The proposed Composite Liquidity Factor (CLF) builds on established work in empirical market microstructure that connects order book shape to execution cost. Hasbrouck’s concept of the *log quote slope*—defined as the rate of price change per unit of depth—serves as a key antecedent [26]. Figure 3 illustrates this slope as the gradient of the line connecting logarithmic quantity and price at the top levels of the bid and ask. As more quantity accumulates near the mid-price, this slope flattens, indicating increased liquidity. Bouchaud et al. [27] and Cont and de Larrard [28] further emphasize how convexity and depth regularities shape price impact and short-term stability. Glosten’s decomposition of spreads into permanent and transitory components [29] also links slope to the informational cost of trading. The CLF adapts these ideas into a direction-sensitive liquidity metric, tailored to identify the more execution-stable reference leg in rollover spreads.

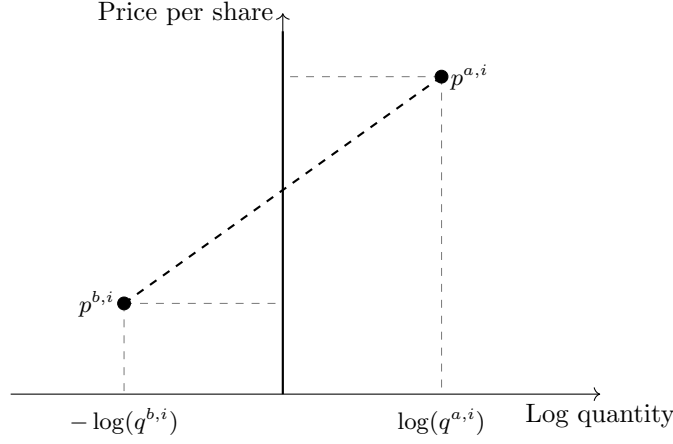


Figure 3: Illustration of the log quote slope: the slope of the dashed line connecting $(-\log(q^{b,i}), p^{b,i})$ and $(\log(q^{a,i}), p^{a,i})$. Adapted from Hasbrouck and Seppi (2001, Fig. 2).

The *log-quote slope* is a well-established measure of liquidity that combines information from the bid-ask spread and the associated quote depth. However, for the purpose of optimally selecting a reference contract in our setting, we are particularly interested in modeling liquidity asymmetries—specifically, discontinuities on a single side of the order book. The relevant side (bid or ask) depends on whether we are initiating a buy or sell spread.

In this paper, we consider the case of futures rollovers as our motivating example. A typical futures rollover strategy involves *buying the spread*, which means selling the current month’s futures contract and simultaneously buying the next month’s contract. To execute this rollover with minimal slippage, it is crucial to evaluate which side—either the bid side of the current month contract or the ask side of the next month contract—offers better instantaneous liquidity for the required quantity.

To this end, we introduce a modified formulation of the log-quote slope tailored to our needs. We refer to this new measure as the **Composite Liquidity Factor (CLF)**. This formulation

retains the essence of the original slope measure but adapts the notation to remain consistent with the rest of the paper.

When using the **current month futures contract** as the reference leg, the CLF is defined as:

$$CLF_c^{b,i} = \frac{\log(p_c^{b,1}/p_c^{b,i+1})}{\log(\sum_{j=1}^i q_c^{b,j})} \quad \forall p_c^{b,i+1} > p_c^{b,i}, i+1 \leq \nu \quad (22)$$

Conversely, when using the **next month futures contract** as the reference leg, the CLF is defined as:

$$CLF_n^{a,i} = \frac{\log(p_n^{a,i+1}/p_n^{a,1})}{\log(\sum_{j=1}^i q_n^{a,j})} \quad \forall p_n^{a,i+1} > p_n^{a,i}, i+1 \leq \nu \quad (23)$$

Here, $p_X^{Y,i}$ represents the price at level i of the relevant side of the order book, and $q_X^{Y,j}$ denotes the aggregated quantity to level j . The numerator captures the logarithmic price drop (or rise), while the denominator aggregates the logarithmic depth over the first i levels. This construction provides a flexible and direction-sensitive indicator of slippage risk, suited to the decision of reference contract selection in spread-based strategies. Unlike the Hawkes-based approach, the CLF-based rule requires no model fitting or simulation. All quantities used in the decision rule are computed directly from the current limit order book snapshot, making the method suitable for real-time application in latency-sensitive environments.

We now define the CLF-based quoting rule formally, using the same decision function structure introduced in Problem 1.2.

Formal Definition: CLF-Based Reference Leg Selection Rule.

For each evaluation window $w = [w_1, w_2) \in \mathcal{W}$, let $\mathcal{G}^B(w) \in \mathbb{R}^2$ denote the book-based filter output containing directional liquidity values for the two contract legs. Define:

$$\begin{aligned} \mathcal{G}^B(w) &:= (CLF_c(w), CLF_n(w)) \\ \mathcal{Q}^B(w) &:= \arg \min_{r \in \{c, n\}} CLF_r(w) \\ \chi^B(w) &:= \mathbb{I}\{\mathcal{Q}^B(w) = n\} \end{aligned}$$

where $CLF_r(w)$ denotes the composite liquidity factor for leg $r \in \{c, n\}$, and n refers to the next-month contract.

This decision rule operates entirely on the book-based filtered representation $\mathcal{G}^B(w)$, requiring no historical data, simulation, or model fitting. It is fully deterministic and computed from observable execution risk at the quoting time w_1 . By capturing asymmetries in directional liquidity across contract legs, $\mathcal{G}^B(w)$ provides a structurally simpler, real-time quoting signal that complements event-driven methods.

The two approaches discussed in this paper reflect different assumptions about the information content of market data. The Hawkes-based rule treats reference-impacting events as informative flow variables, modeling their interactions over time. In contrast, the CLF-based rule assumes that execution-relevant information is embedded in the instantaneous structure of the limit order book. This distinction is not meant to imply any claim about informational efficiency; rather, it frames a practical and philosophical contrast between flow-based and state-based decision systems for short-term execution modeling.

11 Experiment

We now evaluate the reference leg selection rules introduced earlier using high-frequency limit order book data from February 7, 2022, for NIFTY futures contracts expiring in February (F_c) and March (F_n). Each method—Hawkes-based forecasting, CLF-based slope analysis, and the market-optimal benchmark—is assessed within the unified decision framework described in Problem 1.2.

Hawkes-Based Forecasting. The decision rule $\chi^{\mathcal{H}}(w)$, defined in Section 9, uses simulated forward intensities derived from a fitted multivariate Hawkes process. For each rolling window of 1000 ms, we estimate the Hawkes kernels over reference-impacting events—trades, cancellations, and downward price modifications—using maximum likelihood. We then simulate K future realizations over a 10 ms forecast horizon. These simulations yield reference-side event counts, from which arrival ratios $\rho_{(w)}^{X,Y}$ are computed and used to derive the binary decision $\chi^{\mathcal{H}}(w) \in \{0, 1\}$.

CLF-Based Rule. In parallel, we implement the order-book-state-based decision rule $\chi^{\mathcal{B}}(w)$, described in Section 10. At each tick, we compute CLF scores over multiple depths (denoted CLF_1 through CLF_4) for both F_c and F_n . A lower CLF value indicates a more favorable liquidity slope for execution. The contract with the lower CLF is selected at each tick, and a majority vote over the previous 1000 ms determines the decision $\chi^{\mathcal{B}}(w)$ used for the next interval. Ties are resolved in favor of the next-month contract F_n .

Modeling Remark

Although directional liquidity values used in the CLF-based rule are computed at tick resolution, the formal decision framework in Problem 1.2 requires that all quoting rules be evaluated over fixed intervals $w \in \mathcal{W}$. To reconcile this, the book-based filter $\mathcal{G}^{\mathcal{B}}(w) \in \mathbb{R}^2$ is computed by applying an exponential moving average (EMA) to tick-level CLF values observed over the historical window $(w_1 - h, w_1]$. The resulting smoothed features are assumed to remain valid throughout the forecast interval $w = [w_1, w_2)$, and are used to produce a deterministic reference leg decision $\chi^{\mathcal{B}}(w)$.

Market-Optimal Benchmark. Prior to computing the Hawkes based rule and the CLF based rule, we use the method presented in Section 7 to compute a benchmark for evaluation of both rules. We construct a reference oracle $\chi^m(w) \in \{0, 1\}$, which selects the contract that would have yielded the lower realized spread in hindsight. For each window $w \in \mathcal{W}$, we compute the actual execution spreads for both reference leg choices and select the contract that minimizes slippage.

Evaluation Metric. Each method’s prediction accuracy is measured using the agreement score $\mathcal{A}(\chi, \chi^m)$, as defined in Problem 1.2:

$$\mathcal{A}(\chi, \chi^m) := \frac{1}{|\mathcal{W}|} \sum_{w \in \mathcal{W}} \mathbb{I}\{\chi(w) = \chi^m(w)\}$$

This metric reflects how often each rule’s decision matches the market-optimal choice based on realized execution outcomes.

Decision Rule Summary. To contextualize the empirical comparison, we summarize the three decision rules evaluated in this experiment.

Summary of Reference Leg Decision Rules.

Hawkes-based rule: $\chi^{\mathcal{H}}(w) = \mathbb{I} \{ \rho^{c,a}(w) \geq \rho^{n,b}(w) \}$

CLF-based rule: $\chi^{\mathcal{B}}(w) = \mathbb{I} \{ CLF_n(w) < CLF_c(w) \}$

Market-optimal rule: $\chi^m(w) = \arg \min_{r \in \{c,n\}} \delta_S^{(r)}(w)$

This evaluation framework enables a direct comparison of flow-based and state-based decision models under realistic market conditions, using slippage-minimizing outcomes as ground truth.

12 Results

We divide the results into two parts. First, we evaluate the relative predictive performance of different Hawkes kernel specifications using the test for superior predictive ability (SPA). Second, we compare the predictive accuracy of the Hawkes-based reference leg selection rule $\chi^{\mathcal{H}}(w)$ and the CLF-based rule $\chi^{\mathcal{B}}(w)$, both benchmarked against the market-optimal decision $\chi^m(w)$ introduced in Problem 1.2.

12.1 Hawkes Kernel Selection

Table 8 reports SPA test values for four kernel specifications: two parametric (HawkesExp and HawkesSumExp) and two non-parametric (HawkesEM and HawkesCondLaw). The parametric methods yield comparable test values of 0.017 and 0.015, respectively, indicating similar performance. The non-parametric methods exhibit greater variability: the EM-based kernel records a substantially higher test value of 0.530, while the conditional law kernel yields 0.0. These results suggest that the expectation-maximization approach offers superior predictive ability under this test.

Table 8: SPA test values for Hawkes kernel specifications

HawkesExp	HawkesSumExp	HawkesEM	HawkesCondLaw
0.017	0.015	0.530	0.000

Since the SPA test does not reject the null hypothesis that the EM-based kernel is the benchmark, we adopt the HawkesEM specification for all subsequent analyses.

12.2 Comparison of Hawkes Arrival Ratio and CLF

We now compare the Hawkes-based rule $\chi^{\mathcal{H}}(w)$ and the CLF-based rule $\chi^{\mathcal{B}}(w)$ against the market-optimal benchmark $\chi^m(w)$, using the agreement score $\mathcal{A}(\chi, \chi^m)$ defined in Problem 1.2. The evaluation uses high-frequency tick data from February 7, 2022, for NIFTY futures contracts F_c and F_n .

For the Hawkes rule, we fit the expectation-maximization kernel over a rolling 1000 ms window, advanced in 10 ms steps, using only events that impact top-of-book price (trades, cancellations, downward price moves). For each forecast window of 10 ms, we simulate arrival counts and compute arrival ratios $\rho_{(w)}^{X,Y}$, selecting the reference leg via the decision rule defined in Section 9.

The CLF-based rule is evaluated using four variants CLF_1 through CLF_4 , corresponding to increasing quote depth. At each tick, the contract with the lower CLF value is selected. These raw tick-level decisions are smoothed via an exponential moving average over the interval $(\tau - h, \tau]$, as described in the Experiment section, and the resulting signal is used to produce a binary decision $\chi^B(w)$ for each forecast window.

The market-optimal benchmark $\chi^m(w)$ is computed using realized spread over each minute-long interval. The agreement score $\mathcal{A}(\chi, \chi^m)$ is then used to measure the fraction of windows for which each method’s predicted reference leg matches the benchmark.

Table 9: Agreement score $\mathcal{A}(\chi, \chi^m)$: Proportion of windows where predicted reference leg matches market-optimal decision (Feb 7, 2022)

Method	Agreement Score
CLF_1	0.3796
CLF_2	0.4754
CLF_3	0.5919
CLF_4	0.6358
Hawkes Arrival Ratio	0.7335

The results in Table 9 show that the Hawkes arrival ratio significantly outperforms all CLF variants, correctly identifying the optimal reference leg in 73.35% of windows. Among the CLF variants, performance improves with quote depth, with CLF_4 achieving 63.58%, followed by CLF_3 , CLF_2 , and CLF_1 .

These findings highlight the predictive advantage of the Hawkes framework, which models temporal cross-excitation in event arrivals. By capturing dependencies between price-impacting events across contracts and book sides, the Hawkes method provides a dynamic signal for price stability, whereas CLF scores rely on static order book snapshots. This result supports the inclusion of event dynamics in real-time reference leg selection for spread execution strategies.

13 Discussion

This section synthesizes the empirical findings presented in the preceding sections, with particular emphasis on the comparative behavior of reference leg selection rules under realistic quoting and execution scenarios. The evaluation framework was structured to isolate and test three competing decision mechanisms: the *timestamp-based forecast rule* (Hawkes-driven), the *state-based CLF rule*, and the *baseline benchmark rule*.

The forecasting rule derived from Hawkes-based arrival modeling demonstrated clear statistical advantage in periods with stable excitation geometry. This was most evident in the reduced slippage profile during episodes where trade initiations displayed directional clustering. The model’s ability to forecast the relative aggressiveness of future events allowed it to anticipate where liquidity would first disappear, and hence quote accordingly. However, this advantage was attenuated in periods where the order flow exhibited higher randomness or event-type inversion, reducing the predictive signal embedded in the arrival ratio.

In contrast, the CLF rule—by construction—remained robust to such statistical variations. Its performance was governed primarily by the instantaneous imbalance in executable quantity across

price levels, making it a locally optimal, myopic strategy. While it did not benefit from future information encoded in event history, it incurred less variance across market regimes and was notably more stable under low-activity conditions. The deterministic nature of the CLF rule made it computationally tractable and deployable without a learning phase or model calibration.

Across all experiments, the benchmark strategy served as a neutral baseline, confirming that naive quoting can lead to systematically higher slippage, particularly when spread compression or one-sided flow is present.

Modeling Remark. The CLF rule is fully deterministic and real-time computable, requiring only an order book snapshot at decision time.

Importantly, our results point to a broader distinction in modeling philosophy: the Hawkes-based rule exploits temporal structure and historical excitation, whereas the CLF rule is anchored in instantaneous state asymmetry. This distinction reflects an implicit divide between modeling order flow memory (i.e., endogenous clustering) and modeling latent liquidity (i.e., revealed imbalance). The differing slippage behavior of these rules, therefore, encodes more than just execution performance—it also offers insight into how informational content is embedded in different layers of market microstructure.

That said, each model has limitations. The Hawkes-based forecast rule requires reliable estimation of excitation parameters, and may underperform in thin markets where event sparsity limits inference. The CLF rule, while robust, may miss cross-contract signals that are only apparent in temporally coupled dynamics.

We now consolidate these results to outline actionable implications for execution strategy design.

14 Conclusion

This paper examined the impact of reference leg selection on execution quality in calendar spread quoting strategies. By evaluating two distinct decision frameworks—one based on historical excitation patterns (via Hawkes arrival ratios) and the other on contemporaneous order book state (via the Composite Liquidity Factor)—we demonstrated that reference leg choice can materially affect slippage and fill quality, even when quoting spreads are symmetric.

The Hawkes-based forecasting rule proved effective in markets exhibiting persistent excitation geometry, capturing directional order flow and anticipating the side where liquidity would thin out first. In contrast, the CLF rule offered robustness and immediate computability, with stable performance across market regimes, particularly in sparse or noisy environments.

The experimental results reveal that no single quoting strategy dominates across all conditions. Rather, execution performance depends on the interaction between order flow memory and real-time liquidity imbalance. This underscores the need for adaptive quoting logic that blends historical event structure with instantaneous state features.

Future work can explore hybrid strategies that incorporate both Hawkes-based inference and CLF signals, possibly using reinforcement learning to dynamically arbitrate between them. Additionally, incorporating additional market context—such as contract-specific volatility or macroeconomic event markers—may improve the decision framework’s resilience.

References

- [1] Aldridge I. *High-frequency trading: a practical guide to algorithmic strategies and trading systems*. John Wiley & Sons, 2013.
- [2] Brogaard J, Hendershott T and Riordan R. High frequency trading and its impact on market quality. *Journal of Financial Economics* 2014; 113(1): 1–28.
- [3] Clapham B. The impact of high-frequency trading on market stability. *Journal of Financial Markets* 2022; 25: 100–118.
- [4] Kearns M, Kulesza A and Nevmyvaka Y. Empirical limitations on high-frequency trading profitability. *The Journal of Trading* 2010; 5(4): 50–62.
- [5] Hasbrouck J and Saar G. Low-latency trading. *Journal of Financial Markets* 2013; 16(4): 646–679.
- [6] Hull JC. *Options, Futures, and Other Derivatives*. Pearson, 2018.
- [7] Buehlmaier MM. Option spread strategies: An empirical study on risk-return profiles. *Journal of Financial Economics* 2019; 131(2): 456–472.
- [8] Macbeth J. Trading and hedging iron condors in volatile markets. *Financial Analysts Journal* 2011; 67(4): 34–45.
- [9] Bertsimas D and Lo AW. Stochastic programming methods in arbitrage portfolio construction. *Management Science* 2001; 47(3): 455–468.
- [10] Avellaneda M and Stoikov S. High-frequency trading in a limit order book. *Quantitative Finance* 2008; 8(3): 217–224.
- [11] Cartea A, Jaimungal S and Penalva J. *Algorithmic and High-Frequency Trading*. Cambridge University Press, 2015.
- [12] Foucault T, Kadan O and Kandel E. Limit order book as a market for liquidity. *Review of Financial Studies* 2005; 18(4): 1171–1217.
- [13] Bergault P, Evangelista D, Guéant O et al. Closed-form approximations in multi-asset market making. *Applied Mathematical Finance* 2021; 28(2): 101–142.
- [14] Cartea A, Jaimungal S and Penalva J. Buy low, sell high: A high-frequency trading perspective. *Quantitative Finance* 2014; 14(4): 529–546.
- [15] Bacry E, Mastromatteo I and Muzy JF. Hawkes processes in finance. *Market Microstructure and Liquidity* 2015; 1(01): 1550005.
- [16] Hardiman S, Bercot N and Bouchaud JP. Predicting order book dynamics through a self-exciting point process model. *arXiv preprint arXiv:13020133* 2013; .
- [17] Bouchaud JP. *Markets as complex systems*. Cambridge University Press, 2009.
- [18] Cont R, Stoikov S and Talreja R. Price dynamics in a markovian limit order market. *SIAM Journal on Financial Mathematics* 2010; 1(1): 1–25.

- [19] Anantha AN and Jain S. Forecasting high frequency order flow imbalance, 2024. URL <https://arxiv.org/abs/2408.03594>. 2408.03594.
- [20] Ozaki T. Maximum likelihood estimation of hawkes' self-exciting point processes. *Annals of the Institute of Statistical Mathematics* 1979; 31: 145—155.
- [21] Bacry E and Muzy J. Second order statistics characterization of hawkes processes and non-parametric estimation. *arXiv preprint arXiv:14010903* 2014; .
- [22] Lewis E and Mohler G. A non-parametric em algorithm for multiscale hawkes processes. *Journal of Non-Parametric Statistics* 2011; 1(1): 1–20.
- [23] Ogata Y. On lewis' simulation method for point processes. *IEEE transactions on Information Theory* 1981; 27(1): 23–31.
- [24] Hansen P. A test for superior predictive ability. *Journal of Business & Economic Statistics* 2005; 23(4): 365–380.
- [25] Chavez-Demoulin V and McGill J. High-frequency financial data modeling using hawkes processes. *Journal of Banking & Finance* 2012; 36(12): 3415–3426.
- [26] Hasbrouck J and Seppi DJ. Common factors in prices, order flows, and liquidity. *Journal of Financial Economics* 2001; 59(3): 383–411.
- [27] Bouchaud JP, Mezard M and Potters M. Statistical properties of stock order books: empirical results and models. *Quantitative Finance* 2002; 2(4): 251–256.
- [28] Cont R and De Larrard A. Price dynamics in a markovian limit order market. *SIAM Journal on Financial Mathematics* 2014; 4(1): 1–25.
- [29] Glosten LR. Components of the bid-ask spread and the statistical properties of transaction prices. *Journal of Finance* 1987; 42(5): 1293–1307.

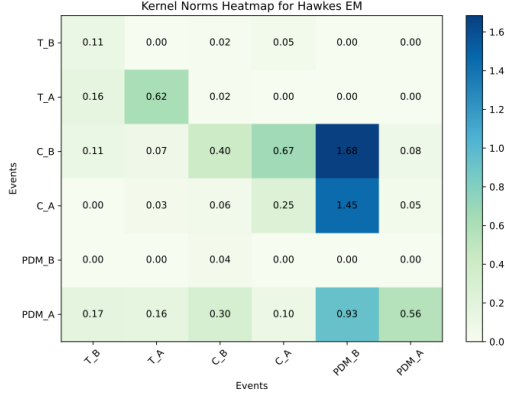
15 Appendix I: Intraday Variation in Excitation Structure

We visualize the Hawkes EM kernel norms across three time blocks to illustrate how excitation strength between event types evolves intraday. Each pair shows the ask and bid sides during a 20-minute window.

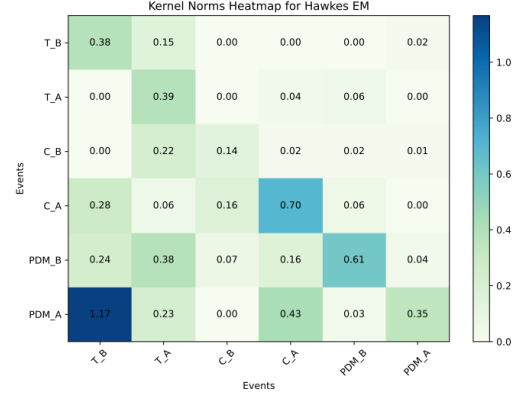
In each pair of kernel norm heat maps shown above, the left heatmap corresponds to the NIFTY futures contract expiring on 24th February 2022, and the right to the contract expiring on 30th March 2022.

Table 10: Microstructure Event Types Used in Hawkes Modeling

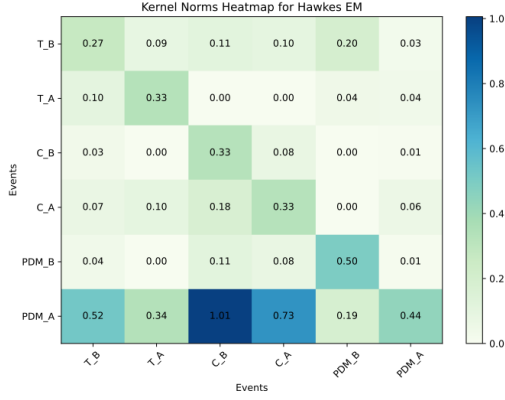
Label	Description
T_A	Trade from aggressive order on the ask.
T_B	Trade from aggressive order on the bid.
C_A	Cancellation at the top level of the ask.
C_B	Cancellation at the top level of the bid.
PDM_A	Downward price adjustment on the ask.
PDM_B	Downward price adjustment on the bid.



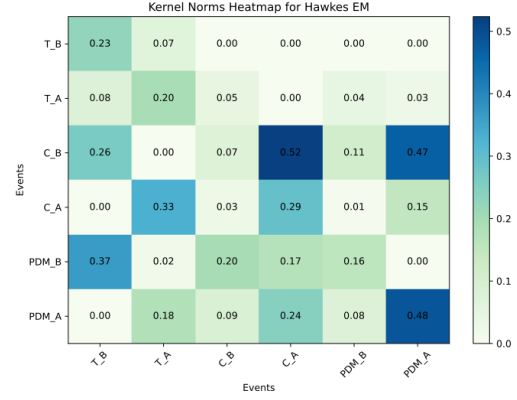
10:05–10:25 AM: NIFTY FEB contract



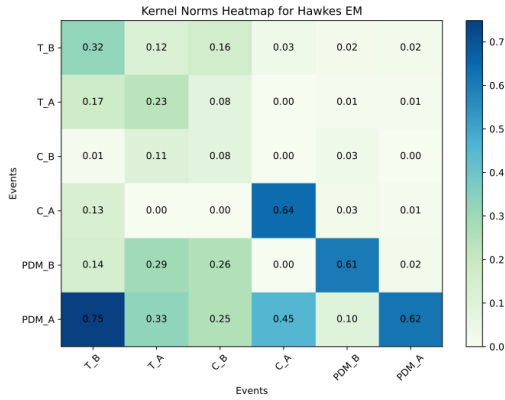
10:05–10:25 AM: NIFTY MAR contract



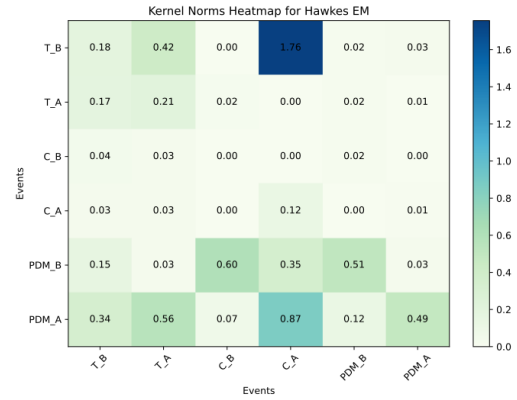
12:10–12:30 PM: NIFTY FEB contract



12:10–12:30 PM: NIFTY MAR contract



2:10–2:30 PM: NIFTY FEB contract



2:10–2:30 PM: NIFTY MAR contract

Figure 4: Pairwise comparison of Hawkes kernel norms across different intraday windows. Each row compares the February and March expiry contracts for the same time block.

16 Appendix II: Sample Tick Data

The table below displays a snippet of the raw tick-by-tick data used in the experiments. It includes timestamps, event types, order sides, price levels, and available quantities. This example illustrates the granularity and structure of the input used to estimate Hawkes kernels and compute liquidity metrics.

Server_epoch_nanos	Symbol	event_type	side	Price	Qty	OID1	OID2	Agg	capture_timestampz
1644227998953429992	NSEFNO_NIFTY_G22	TRADE		17214.00	50	1100000071295344	1100000071290667	BUY	2022-02-07 09:59:58.953429992+00
1644227999031664383	NSEFNO_NIFTY_G22	TRADE		17213.80	50	1100000071295449	1100000071295363	BUY	2022-02-07 09:59:59.031664383+00
1644227999031664383	NSEFNO_NIFTY_G22	TRADE		17213.85	150	1100000071295449	1100000071290493	BUY	2022-02-07 09:59:59.031664383+00
1644205500049497674	NSEFNO_NIFTY_G22	N	BUY	17000.00	50	1100000000001754			2022-02-07 03:45:00.049497674+00
1644205500050566579	NSEFNO_NIFTY_G22	N	BUY	17401.10	100	1100000000001939			2022-02-07 03:45:00.050566579+00
1644205500050579855	NSEFNO_NIFTY_G22	N	BUY	16901.05	100	1100000000001941			2022-02-07 03:45:00.050579855+00
1644205500050016996	NSEFNO_NIFTY_G22	N	SELL	17460.00	50	1100000000001849			2022-02-07 03:45:00.050016996+00
1644205500050096128	NSEFNO_NIFTY_G22	N	SELL	17500.00	100	1100000000001864			2022-02-07 03:45:00.050096128+00
1644205500050121328	NSEFNO_NIFTY_G22	N	SELL	17458.55	400	1100000000001868			2022-02-07 03:45:00.050121328+00
1644227999966936439	NSEFNO_NIFTY_G22	MODIFY_TICK	SELL	17225.00	250	1100000045070355			2022-02-07 09:59:59.966936439+00
1644227999969919000	NSEFNO_NIFTY_G22	MODIFY_TICK	BUY	17205.95	100	1100000071271630			2022-02-07 09:59:59.969919000+00
1644227999988916651	NSEFNO_NIFTY_G22	MODIFY_TICK	SELL	17216.70	100	1100000071286370			2022-02-07 09:59:59.988916651+00
1644228205338970644	NSEFNO_NIFTY_G22	CANCEL_TICK	SELL	17444.00	50	1100000012222592			2022-02-07 10:03:25.338970644+00
1644228205340990944	NSEFNO_NIFTY_G22	CANCEL_TICK	SELL	17273.00	50	1100000010068455			2022-02-07 10:03:25.340990944+00
1644228205341822198	NSEFNO_NIFTY_G22	CANCEL_TICK	BUY	17000.00	550	1100000058552827			2022-02-07 10:03:25.341822198+00

Table 11: Data Snippet of Date 20220207 ('TRADE': trade tick order, 'N': new tick order, 'MODIFY_TICK': modification tick order, 'CANCEL_TICK': cancellation tick order)

17 Appendix III: Global Notation Summary

Table 12: Summary of Symbols and Their First Point of Introduction

Symbol	Description	Section
<i>Market Structure and Events</i>		
F_c, F_n	Current and next-month futures contracts	Problem Formulation
$p^{b,i}, p^{a,i}$	Price at level i on bid / ask side	CLF Section
$q^{b,i}, q^{a,i}$	Quantity at level i on bid / ask side	CLF Section
$X \in \{c, n\}$	Contract index: current or next-month	Forecasting Objective
$Y \in \{b, a\}$	Order book side: bid or ask	Forecasting Objective
\mathcal{E}	Event types: trades (T), cancels (C), PDM	Forecasting Objective
\mathcal{I}	Index set for Hawkes dimensions	Forecasting Objective
T_A, T_B	Trades due to aggressive orders on ask/bid	Appendix Table
C_A, C_B	Cancellations at top of ask/bid	Appendix Table
PDM_A, PDM_B	Price-down moves on ask/bid side	Appendix Table
<i>Feature Extraction and Data Structures</i>		
$\mathcal{T}(w)$	Tick history in interval w	Problem Formulation
$\mathcal{B}(w)$	LOB snapshot at start of window w	Problem Formulation
\mathcal{W}	Set of all evaluation windows $w = [\tau, \tau + \xi)$	Problem Formulation
τ	Start time of evaluation window w	Problem Formulation
ξ	Forecast horizon length	Problem Formulation
$\mathcal{K}^{\mathcal{T}}, \mathcal{K}^{\mathcal{B}}, \mathcal{K}^{\mathcal{H}}$	Feature extraction maps from tick, book, and Hawkes data	Problem Formulation
$\mathcal{G}^{\mathcal{T}}, \mathcal{G}^{\mathcal{B}}, \mathcal{G}^{\mathcal{H}}$	Resulting feature vectors from each input source	Problem Formulation
<i>Decision Rules and Outcomes</i>		
$\mathcal{Q}^{\mathcal{T}}, \mathcal{Q}^{\mathcal{B}}, \mathcal{Q}^{\mathcal{H}}$	Scoring functions mapping features to reference leg choices	Problem Formulation
$\chi^{\mathcal{T}}(w), \chi^{\mathcal{B}}(w), \chi^{\mathcal{H}}(w)$	Binary decisions: $0 = F_c, 1 = F_n$	Problem Formulation
$\chi^m(w)$	Market-optimal reference leg (minimum realized spread)	Problem Formulation
<i>Hawkes Process Components</i>		
λ_t^i	Intensity function for event type i	Hawkes Forecasting
μ^i	Baseline intensity for event type i	Hawkes Forecasting
$\phi_{ij}(t)$	Kernel function: excitation from j to i	Hawkes Forecasting
$\tilde{N}_{(w)}^{X,Y}$	Simulated total event count over window w	Forecasting Objective
$\tilde{N}_{(w)}^{X,Y,r}$	Simulated reference-impacting event count	Forecasting Objective
$\rho_{(w)}^{X,Y}$	Arrival ratio: $\tilde{N}_{(w)}^{X,Y,r} / \tilde{N}_{(w)}^{X,Y}$	Forecasting Objective
<i>Liquidity and Evaluation Metrics</i>		
CLF_i	Composite Liquidity Factor using top i LOB levels	CLF Section
$\delta_S^{(r)}(w)$	Realized spread under contract r as reference leg	Problem Formulation
$\mathcal{A}(\chi, \chi^m)$	Agreement score: $\frac{1}{ \mathcal{W} } \sum \mathbb{I}\{\chi(w) = \chi^m(w)\}$	Problem Formulation